Charge-state distribution of ^{238}U in nitrogen gas and carbon foil at 14 and 15 MeV/nucleon

H. Kuboki,* H. Okuno, H. Hasebe, S. Yokouchi, N. Fukunishi, Y. Higurashi, J. Ohnishi, T. Nakagawa, H. Imao, O. Kamigaito, A. Goto, M. Kase, and Y. Yano

RIKEN Nishina Center for Accelerator-Based Science, Wako, Saitama 351-0198, Japan

(Received 9 February 2011; published 31 May 2011)

The charge-state distributions of ^{238}U with energies of 14 and 15 MeV/nucleon were measured using nitrogen (N_2) gas and carbon foil (C-foil) charge strippers. The most probable charge states of ^{238}U with energies of 14 and 15 MeV/nucleon in N_2 gas attain equilibrium at 60.8 and 62.4, whereas those in C-foils attain equilibrium at 75.8 and 76.7, respectively. Novel empirical formulas for the accurate prediction of the equilibrium charge states of ^{238}U with energies 10–20 MeV/nucleon in gases and C-foil were derived by fitting the data in the energy range of 1–20 MeV/nucleon. The charge states predicted by using the formulas for gases and C-foil are in good agreement with the data in the energy range of 10–20 MeV/nucleon within an average of 0.23 and 0.21, respectively.

DOI: 10.1103/PhysRevSTAB.14.053502 PACS numbers: 29.20.dg, 29.25.Pj, 34.50.Fa

I. INTRODUCTION

The charge states of heavy ion beams play an important role in the performance of heavy ion accelerators. To realize efficient acceleration of heavy ions such as uranium up to high energies, prediction of the charge states is crucial for the design of accelerators, especially at energies of 10–20 MeV/nucleon, where charge strippers are commonly used. The stripping energies of uranium ion beams are 11 MeV/nucleon at the RIKEN RI Beam Factory (RIBF) [1] and GSI [2], and 16.5 MeV/nucleon at FRIB [3]. In this energy range, 20–40 electrons of the uranium ions are stripped after passage through the charge-stripping materials, and the charge states of the stripped beams are considerably enhanced. However, a large number of electrons are involved in the charge-stripping process; hence, the empirically predicted charge states of uranium are highly ambiguous at the stripping energies. Recently, we measured the equilibrium charge states of uranium (^{238}U) ion beams in gases and carbon foils (C-foils) at 11 MeV/nucleon [1,4]; for the first time, the equilibrium charge states of ^{238}U in gases were measured at an energy of around 10 MeV/nucleon using nitrogen (N_2), argon (Ar), and CO_2 gas charge strippers [4]. An empirical formula for the prediction of the equilibrium charge state in gaseous media was derived by fitting the data over the energy range of 0.01–60 MeV/nucleon [4]. However, among the data sets used for fitting, 11 MeV/nucleon was the only available energy in the range of 10–20 MeV/nucleon. Moreover, it was unclear whether the empirical formula based on data over such a broad energy range (0.01–60 MeV/nucleon) could be applied to accurately predict the charge states within 1 charge unit at other energies in the range of 10–20 MeV/nucleon. In the case of C-foils, only two data sets of uranium charge states were available [1,5] in the energy range of 10–20 MeV/nucleon. It is necessary to employ experimental data at other energies in this range in order to improve the accuracy of the empirical formulas.

Therefore, in the present study, we measured the charge-state distributions of ^{238}U at 14 and 15 MeV/nucleon using N_2 gas and C-foils with different thicknesses. Additional data were obtained for the charge-state distribution at 11 MeV/nucleon in order to examine the validity of the previous results. Empirical formulas were derived by fitting the systematic data sets obtained in this study as well as those previously obtained in the energy range of 1–20 MeV/nucleon. Finally, we improved the accuracy of the empirical formulas for prediction of the equilibrium charge states in gases and C-foils in the energy range of 10–20 MeV/nucleon.

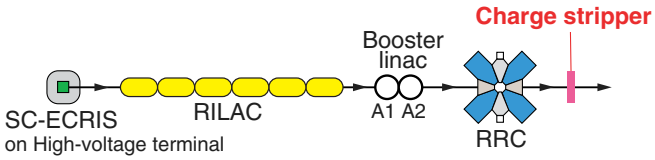

FIG. 1. Acceleration scheme of the experiment. The charge stripper is located downstream of the RRC. The uranium ions were extracted from the SC-ECRIS on the high-voltage platform of the Cockcroft-Walton preinjector in the RILAC facility. The first two resonators (A1 and A2) of the booster linac were used for the beam energies of 14 and 15 MeV/nucleon, where the RRC was operated at the harmonic number of $h = 8$.

*kuboki@riken.jp

TABLE I. Parameters of acceleration modes of uranium beams.

RRC output energy (MeV/nucleon)	11	14	15
RILAC and RRC frequency (MHz)	18.25	18.25	19.00
Booster frequency (MHz)	(not used)	36.50	38.00
RRC harmonic number (h)	9	8	8
Charge state at SC-ECRIS	35	41	41
Beam intensity at SC-ECRIS (eμA)	10–12	1.5–2.0	2.4–2.6
Total voltage at entrance of RILAC (kV)	127	109	118

II. EXPERIMENTS AND RESULTS

A. Uranium acceleration

The experiments were performed at the RIKEN RIBF by accelerating the uranium beams through the RIKEN heavy ion linac (RILAC) [6], booster linac [7], and RIKEN ring cyclotron (RRC) [8,9], as shown schematically in Fig. 1. The highly charged ions of ^{238}U were provided by the superconducting electron-cyclotron-resonance ion source (SC-ECRIS) [10–12], which had been placed on the high-voltage terminal of the Cockcroft-Walton preinjector of the RILAC [13]. We tuned the beam energies from the RRC by changing the rf frequency of the RILAC, booster, and RRC as well as the harmonic number h of the RRC, as explained below. The nominal beam energy from the RRC for uranium acceleration at the RIBF is 11 MeV/nucleon, which corresponds to an rf frequency of 18.25 MHz and harmonic number of $h = 9$. The booster linac is not used in this acceleration mode. We extracted 10–12 eμA of U^{35+} from the SC-ECRIS, which is acceptable by the RRC in this mode. For the beam energy of 14 MeV/nucleon, we used the first two resonators (A1 and A2) of the booster linac to operate the RRC with the harmonic number of $h = 8$ [14]. The rf frequency of the RRC is 18.25 MHz. Owing to the high performance of the SC-ECRIS, we could extract 1.5–2.0 eμA of the uranium 41+ beam, which is acceptable by the RRC in this acceleration condition. Finally, we tuned the rf frequency of the RRC to 19 MHz in the $h = 8$ mode for the beam energy of 15 MeV/nucleon. The charge state of 41+ is also acceptable by the RRC. The parameters of these acceleration modes are listed in Table I.

B. Charge-state distribution measurement using N_2 gas charge stripper

The ^{238}U beams at 11, 14, and 15 MeV/nucleon were transported to the gas charge stripper [4,15] located upstream of a fixed-frequency ring cyclotron (fRC) [16,17], as shown in Fig. 2. The incident beam intensities were measured using a Faraday cup (FC-D17) placed upstream of the gas charge stripper, and they were measured to be 43, 2.9, and 5.3 pnA for ^{238}U beams with energies of 11, 14, and 15 MeV/nucleon, respectively. The beam spot was 6 mm in diameter, which was comparable to the diameter of the aperture at the entrance of the gas charge stripper.

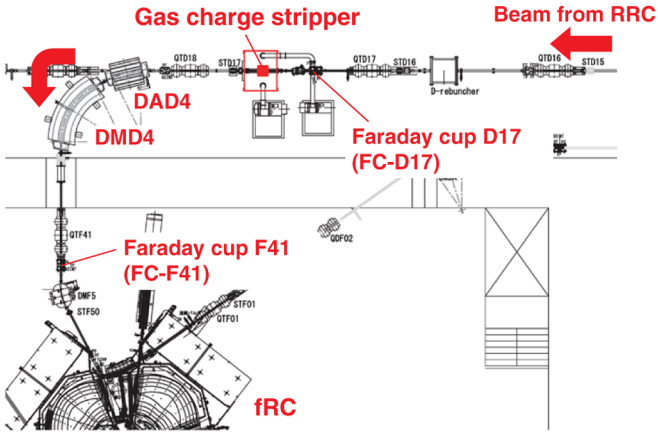

FIG. 2. Schematic view of the beam line around the gas charge stripper. The beam intensity upstream of the gas charge stripper was measured using a Faraday cup (FC-D17). Stripped beams were analyzed using a pair of dipole magnets DAD4 and DMD4. The beam intensity downstream of DAD4 and DMD4 was measured using a Faraday cup (FC-F41).

The charge state was analyzed using the dipole magnets DAD4 and DMD4. The resolving power R of DAD4 and DMD4 was 4.35 cm/% as calculated using the formula $R = |D/M_x|$, where D and M_x denote the dispersion and the horizontal magnification, respectively. The magnetic

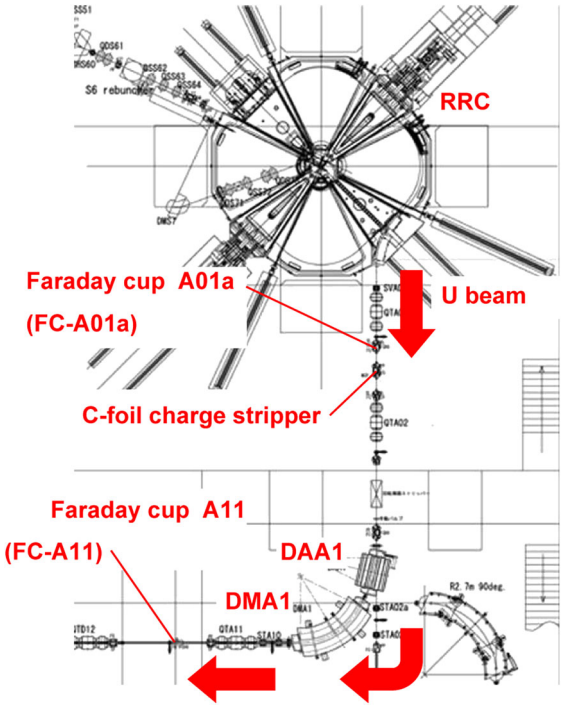

FIG. 3. Schematic view of the beam line around the C-foil charge stripper. The beam intensity upstream of the C-foil charge stripper was measured using a Faraday cup (FC-A01a). Stripped beams were analyzed using a pair of dipole magnets DAA1 and DMA1. The beam intensity downstream of DAA1 and DMA1 was measured using a Faraday cup (FC-A11).

field of these magnets was corrected by taking into account the energy loss in the gas so that a stripped beam in a single charge state passed through the center of the beam line. The beam profile was monitored at 4.8 m downstream of DMD4. The horizontal and vertical beam widths were, at most, 20 and 27 mm, respectively, in 4 standard deviations. The intensities of the stripped beams were measured using a Faraday cup (FC-F41) located 4.9 m downstream of DMD4. The aperture at the entrance of FC-F41 was 36 mm in diameter. The resolving power of DAD4 and DMD4 was sufficiently high compared with the beam width, and thus, there was no contribution from beams in the neighboring charge states.

C. Charge-state distribution measurement using C-foil charge stripper

Figure 3 shows an overview of the beam line around the C-foil charge stripper located downstream of the RRC. The incident beam intensities were measured using a Faraday cup (FC-A01a) placed upstream of the C-foil charge stripper, and they were measured to be 51, 2.4, and 7.9 pnA for ^{238}U beams at 11, 14, and 15 MeV/nucleon, respectively. The beam intensities were attenuated accordingly in order to reduce irradiation damage to the C-foils. The beam spot was 5 mm in diameter. The C-foils were purchased from ACF-Metals, Inc. [18]. The charge state was analyzed using the dipole magnets DAA1 and DMA1. The resolving power of DAA1 and DMA1 was $R = 4.35$ cm/%, which was the same as that of DAD4 and DMD4. The magnetic field of these magnets was corrected by taking into account the energy loss in the C-foils in the same way as that used for the gas charge stripper. The beam profile was monitored at 3.4 m downstream of DMA1. The horizontal and vertical beam widths were, at most, 30 and 9 mm, respectively, in 4 standard deviations. The intensities of the stripped beams were measured using a Faraday cup (FC-A11) located 4.7 m downstream of DMA1. The aperture at the entrance of FC-A11 was 62 mm in diameter. As in the case of the gas charge stripper, there was no contribution from beams in the neighboring charge states.

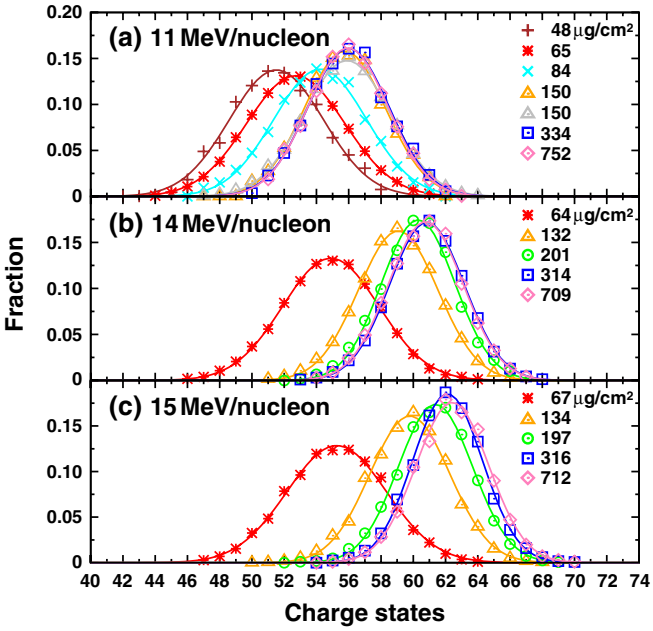

FIG. 4. Charge-state distributions of ^{238}U at different energies measured using the N_2 gas charge stripper. The data of the fractions calculated for (a) 11, (b) 14, and (c) 15 MeV/nucleon are plotted. (a) The data for stripper thicknesses of 48, 65, 84, 150, 334, and 752 μg/cm^2 at 11 MeV/nucleon are denoted by crosses, asterisks, x marks, open triangles, open squares, and open diamonds, respectively. The data for stripper thicknesses of 48, 84, 334, and 752 μg/cm^2 along with one data set of 150 μg/cm^2 were obtained from a previous study [4]. (b) The data for stripper thicknesses of 64, 132, 201, 314, and 709 μg/cm^2 at 14 MeV/nucleon are denoted by asterisks, open triangles, open circles, open squares, and open diamonds, respectively. (c) The data for stripper thicknesses of 67, 134, 197, 316, and 712 μg/cm^2 at 15 MeV/nucleon are denoted by asterisks, open triangles, open circles, open squares, and open diamonds, respectively.

D. Results

The charge-state distributions of ^{238}U measured using the N_2 gas and the C-foil charge strippers with different thicknesses are shown in Figs. 4 and 5, respectively. The gas thickness was calibrated in a previous study [4].

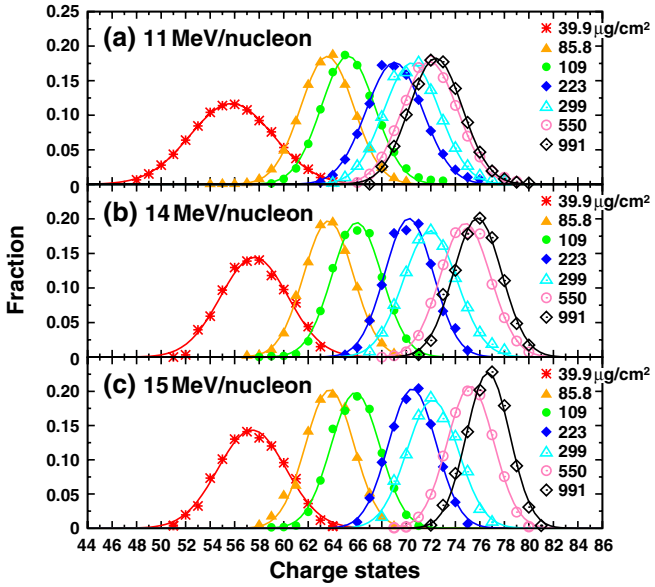

FIG. 5. Charge-state distributions of ^{238}U at different energies measured using the C-foil charge stripper. The data for stripper thicknesses of 39.9, 85.8, 109, 223, 299, 550, and 991 μg/cm^2 are denoted by asterisks, solid triangles, solid circles, solid diamonds, open triangles, open circles, and open diamonds, respectively. The values of the fractions calculated for (a) 11, (b) 14, and (c) 15 MeV/nucleon are plotted.

TABLE II. Fitting parameters of ^{238}U charge-state distributions using the N_2 gas charge stripper. The listed errors are attributed to the fitting procedure. Previous results [4] are included in the list for 11 MeV/nucleon.

Pressure (kPa)	Thickness (μg/cm^2)	Peak height	Center	σ	Ref.
11 MeV/nucleon					
0.29	48 ± 3	0.137 ± 0.003	51.52 ± 0.07	2.92 ± 0.07	[4]
0.39	65 ± 3	0.131 ± 0.001	52.71 ± 0.02	3.04 ± 0.02	
0.50	84 ± 3	0.139 ± 0.002	54.23 ± 0.05	2.87 ± 0.05	[4]
0.90	150 ± 3	0.158 ± 0.003	55.76 ± 0.05	2.53 ± 0.05	[4]
0.90	150 ± 3	0.148 ± 0.002	55.90 ± 0.03	2.71 ± 0.04	
2.00	334 ± 4	0.159 ± 0.003	55.99 ± 0.06	2.51 ± 0.06	[4]
4.50	752 ± 6	0.161 ± 0.002	55.95 ± 0.04	2.47 ± 0.04	[4]
14 MeV/nucleon					
0.38	64 ± 3	0.133 ± 0.001	54.90 ± 0.03	3.01 ± 0.03	
0.79	132 ± 3	0.162 ± 0.002	59.07 ± 0.03	2.47 ± 0.04	
1.20	201 ± 3	0.175 ± 0.004	60.31 ± 0.06	2.25 ± 0.07	
1.88	314 ± 4	0.172 ± 0.001	60.86 ± 0.02	2.33 ± 0.03	
4.24	709 ± 5	0.172 ± 0.003	60.78 ± 0.05	2.32 ± 0.06	
15 MeV/nucleon					
0.40	67 ± 3	0.128 ± 0.002	55.26 ± 0.06	3.11 ± 0.06	
0.80	134 ± 3	0.161 ± 0.003	59.80 ± 0.06	2.48 ± 0.07	
1.18	197 ± 3	0.174 ± 0.003	61.39 ± 0.05	2.30 ± 0.05	
1.89	316 ± 4	0.186 ± 0.004	62.13 ± 0.05	2.15 ± 0.06	
4.26	712 ± 5	0.176 ± 0.004	62.43 ± 0.07	2.27 ± 0.07	

The fraction of charge state q_i was calculated as described in a previous study [4]; it is defined as

$$F(q_i) = \frac{1}{N}\frac{I_{\mathrm{down}}/q_i}{I_{\mathrm{up}}/q_{\mathrm{ini}}}, \quad (1)$$

where N denotes a normalization constant, I_{down} denotes beam intensities downstream of the gas or C-foil charge stripper (measured using FC-F41 or FC-A11), I_{up} denotes beam intensities measured upstream of the gas or C-foil charge stripper (measured using FC-D17 or FC-A01a), and q_{ini} denotes the charge state extracted from the ion source (see Table I). In order to determine N, an unnormalized fraction $f(q_i) = (I_{\mathrm{down}}/q_i)/(I_{\mathrm{up}}/q_{\mathrm{ini}})$ was calculated. The data set of $f(q_i)$ is fitted by a Gaussian function. However, the beam intensity measured using each Faraday cup includes its own offset value; hence, the sum $\sum f(q_i)$ over all i does not equal unity. Therefore, the area of the fitted Gaussian function is calculated and introduced as a normalization constant N in order to obtain the sum of $F(q_i)$ as unity. Then, the set of $F(q_i)$ is fitted by a Gaussian function again. The most probable charge states are defined as the central values obtained by the fitting procedure. The fitted parameters for the N_2 gas and C-foil charge strippers are listed in Tables II and III, respectively. It was found that the most probable charge states in the case of N_2 gas attain equilibrium at 56.0, 60.8, and 62.4 with energies of 11, 14, and 15 MeV/nucleon, respectively. The equilibrium charge state of ^{238}U in N_2 gas at 11 MeV/nucleon is in good agreement with the data from a previous study [4]. The most probable charge states in the case of C-foils attain equilibrium at 72.4, 75.8, and 76.7 with energies of 11, 14, and 15 MeV/nucleon, respectively. The equilibrium charge state of ^{238}U in C-foil at 11 MeV/nucleon is in good agreement with the data from a previous study [1].

Figure 6 shows the most probable charge states plotted as a function of the N_2 gas and C-foil thickness t. The data

TABLE III. Fitting parameters of ^{238}U charge-state distributions using the C-foil charge stripper. The listed errors are attributed to the fitting procedure.

Thickness (μg/cm^2)	Peak height	Center	σ
11 MeV/nucleon			
39.9	0.117 ± 0.001	55.75 ± 0.02	3.42 ± 0.03
85.8	0.185 ± 0.002	63.55 ± 0.03	2.16 ± 0.03
109	0.187 ± 0.003	65.22 ± 0.04	2.13 ± 0.04
223	0.177 ± 0.004	69.01 ± 0.06	2.28 ± 0.07
299	0.176 ± 0.005	70.43 ± 0.07	2.26 ± 0.07
550	0.179 ± 0.002	71.89 ± 0.03	2.23 ± 0.03
991	0.182 ± 0.001	72.40 ± 0.02	2.19 ± 0.02
14 MeV/nucleon			
39.9	0.143 ± 0.005	57.61 ± 0.11	2.81 ± 0.12
85.8	0.197 ± 0.003	63.65 ± 0.04	2.03 ± 0.04
109	0.194 ± 0.005	65.97 ± 0.06	2.06 ± 0.07
223	0.202 ± 0.007	70.20 ± 0.08	1.94 ± 0.09
299	0.183 ± 0.002	71.92 ± 0.02	2.18 ± 0.03
550	0.193 ± 0.006	74.82 ± 0.08	2.07 ± 0.08
991	0.200 ± 0.007	75.81 ± 0.08	1.99 ± 0.08
15 MeV/nucleon			
39.9	0.142 ± 0.003	57.44 ± 0.08	2.84 ± 0.09
85.8	0.202 ± 0.007	63.77 ± 0.08	1.97 ± 0.09
109	0.197 ± 0.006	65.85 ± 0.08	2.03 ± 0.08
223	0.202 ± 0.004	70.51 ± 0.05	2.00 ± 0.06
299	0.186 ± 0.006	72.18 ± 0.08	2.15 ± 0.10
550	0.206 ± 0.002	75.26 ± 0.02	1.94 ± 0.02
991	0.225 ± 0.006	76.70 ± 0.06	1.81 ± 0.06

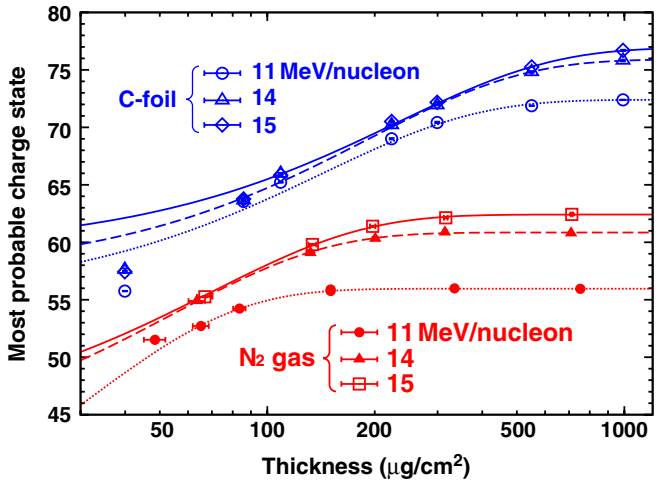

FIG. 6. Most probable charge states of ^{238}U plotted as a function of N_2 gas and C-foil thickness. The data for N_2 gas at 11, 14, and 15 MeV/nucleon are represented by solid circles, solid triangles, and open squares, respectively. Fitting functions are represented by dotted, dashed, and solid curves at 11, 14, and 15 MeV/nucleon, respectively. The data for C-foils at 11, 14, and 15 MeV/nucleon are represented by open circles, open triangles, and open diamonds, respectively. Fitting functions are represented by dotted, dashed, and solid curves at 11, 14, and 15 MeV/nucleon, respectively.

were fitted by a function $f(t) = a - b\exp(-ct)$ in order to calculate the thickness required for the equilibrium charge state, where a, b, and c are fitting parameters. The equilibrium value of the most probable charge state is denoted by a. Parameters b and c denote the quantities related to the thickness required for equilibrium and the slope of the curve before equilibrium, respectively. According to previous results, the thicknesses required for equilibrium at 11 MeV/nucleon are 125 μg/cm^2 and 500 μg/cm^2 for N_2 gas and C-foil, respectively [1,4]. The thicknesses required for equilibrium charge states at 14 and 15 MeV/nucleon are greater than those at 11 MeV/nucleon. Therefore, among the data sets in this study, the data obtained using thicker charge strippers are more important for estimating the thickness for equilibrium. Here, the fitting procedure was carried out to minimize a modified χ^2 value defined as

$$\chi^2 \equiv \sum_i \frac{\{f(t_i) - y_i\}^2 \cdot t_i}{\delta y_i^2},$$

where t_i, y_i, and δy_i denote the thickness, most probable charge state, and its error, the values of which are listed in Tables II and III for the N_2 gas and C-foil charge strippers, respectively. Thus, the ordinary χ^2 term $\{f(t) - y_i\}^2/\delta y_i^2$ is weighted by each thickness value. The obtained parameters are listed in Table IV. The N_2 gas thicknesses required for equilibrium, as calculated by $f(t)$, are 118, 188, and 235 μg/cm^2 at 11, 14, and 15 MeV/nucleon, respectively, whereas the C-foil thicknesses are 454, 617, and 728 μg/cm^2 at 11, 14, and 15 MeV/nucleon, respectively. Here, the thickness required for equilibrium is defined as the thickness required for attaining 99% of the equilibrium charge state.

III. EMPIRICAL FORMULAS

Empirical formulas were obtained by fitting the data in the energy range of 1–20 MeV/nucleon. The fitting procedure is carried out for the data obtained using N_2, Ar, and CO_2 gases ([4,19,20] and this study), and C-foil ([1,19–22] and this study). The data are fitted using the function [4,23]

$$q_{\mathrm{eq}} = Z\left[1 - C\exp\left\{-\left(\frac{v}{v_0}\right)^{\delta} Z^{-\gamma}\right\}\right], \qquad (2)$$

where q_{eq}, Z, v, and v_0 denote the equilibrium charge state, projectile atomic number, projectile velocity, and Bohr velocity of 2.188×10^8 cm/s, respectively. C, δ, and γ are the fitting parameters of the function. The values of the fitting parameters are listed in Table V.

The data in the energy range of 1–20 MeV/nucleon are plotted along with the empirical formulas for (a) gases and (b) C-foil in Fig. 7. In addition to this study, empirical formulas for predicting the charge state in gases have been proposed by Kuboki *et al.* [4], whereas those for predicting

TABLE IV. Fitting parameters of $f(t)$ for ^{238}U are shown together with the thickness required for equilibrium. The equilibrium value of the most probable charge state is denoted by a. Parameter b is related to the thickness required for equilibrium. Parameter c denotes the slope of the curve before equilibrium.

Energy (MeV/nucleon)	a	b	c	Equilibrium thickness (μg/cm^2)
N_2 gas				
11	55.96	27.10	0.033	118.3
14	60.85	19.32	0.018	187.9
15	62.41	18.41	0.014	235.0
C-foil				
11	72.40	17.41	0.0070	454.3
14	75.91	18.80	0.0052	617.2
15	76.92	17.57	0.0043	727.6

TABLE V. Values of the fitting parameters C, δ, and γ for the fitting function q_{eq} in this study.

	C	δ	γ
Gas	0.784	1.63	1.17
C-foil	0.835	1.20	0.736

the charge state in solid materials have been proposed by Leon *et al.* [24], Baron *et al.* [5], McMahan *et al.* [25,26], Schiwietz *et al.* [27], and Strehl [28]. The difference between the predicted values and the data is defined as $\Delta q \equiv \mid q_{\mathrm{eq}}^{\mathrm{exp}} - q_{\mathrm{eq}}^{\mathrm{cal}} \mid$, where $q_{\mathrm{eq}}^{\mathrm{exp}}$ and $q_{\mathrm{eq}}^{\mathrm{cal}}$ denote the experimental data and predicted values of the most probable charge states at equilibrium, respectively. Δq is calculated for each datum in the energy range of 10–20 MeV/nucleon, and it is found that the averaged Δq values are 0.23 and 0.21 for gases and C-foil, respectively.

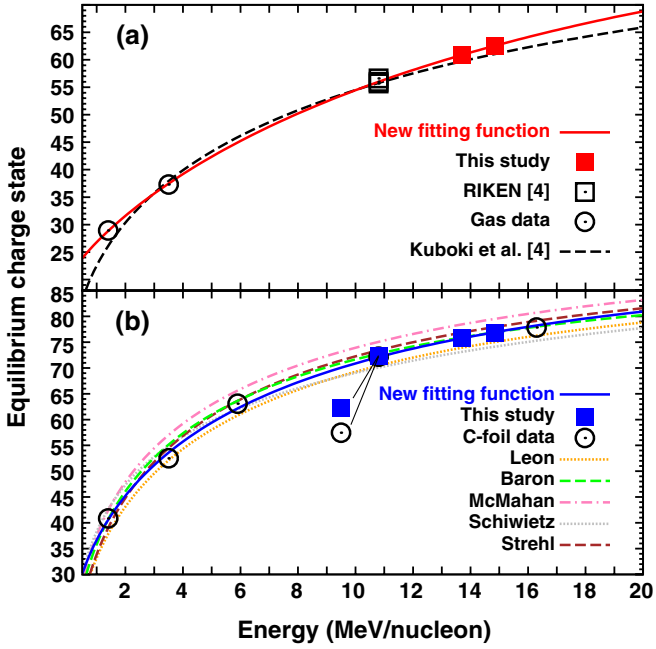

FIG. 7. Data of the equilibrium charge state of uranium ions in (a) N_2, Ar, and CO_2 gases [4,19,20] and (b) C-foil [1,19–22] in the energy range of 1–20 MeV/nucleon. (a) Solid squares represent the data obtained in this study. Open squares represent the results of previous measurements [4]. Open circles represent the data for gases [19,20]. The equilibrium charge states in gases, as predicted by the new fitting function $q_{\mathrm{eq}}^{\mathrm{gas}} = Z[1 - 0.784\ \exp\{-(v/v_0)^{1.63}Z^{-1.17}\}]$ are represented by the solid curve. The dashed curve represents the charge states predicted using the empirical formula [4]. (b) The data obtained in this study is represented by solid squares. Open circles represent the data available for C-foil [1,19–22]. The data at 11 MeV/nucleon obtained in this study is in good agreement with previous data [1]. The blue, orange, green, magenta, gray, and brown curves represent the charge states for solid materials, as predicted by the empirical formulas proposed by us, i.e., $q_{\mathrm{eq}}^{\mathrm{C\text{-}foil}} = Z[1 - 0.835\ \exp\{-(v/v_0)^{1.20}Z^{-0.736}\}]$, Leon *et al.* [24], Baron *et al.* [5], McMahan *et al.* [25,26], Schiwietz *et al.* [27], and Strehl [28], respectively.

IV. SUMMARY AND CONCLUSIONS

We measured the charge-state distributions of ^{238}U at 11, 14, and 15 MeV/nucleon using N_2 gas and C-foil charge strippers. The most probable charge states of ^{238}U with energies of 14 and 15 MeV/nucleon in N_2 gas attain equilibrium at 60.8 and 62.4, respectively, whereas those in C-foils attain equilibrium at 75.8 and 76.7, respectively. The charge state of ^{238}U in C-foil at 11 MeV/nucleon is consistent with the previous data [1]. The N_2 gas thicknesses required for the most probable charge states to attain equilibrium are 118, 188, and 235 μg/cm^2 at 11, 14, and 15 MeV/nucleon, respectively; the corresponding thicknesses for C-foil are 454, 617, and 728 μg/cm^2, respectively. The empirical formula for predicting charge states of ^{238}U in gases in the energy range of 10–20 MeV/nucleon is determined to be $q_{\mathrm{eq}}^{\mathrm{gas}} = Z[1 - 0.784\ \exp\{-(v/v_0)^{1.63}Z^{-1.17}\}]$. The difference between the predicted values and the data, Δq, is averaged over the energy range of 10–20 MeV/nucleon, and its value is found to be 0.23. The empirical formula for C-foil was also obtained, and it is determined to be $q_{\mathrm{eq}}^{\mathrm{C\text{-}foil}} = Z[1 - 0.835\ \exp\{-(v/v_0)^{1.20}Z^{-0.736}\}]$; the averaged Δq over the energy range of 10–20 MeV/nucleon is 0.21.

ACKNOWLEDGMENTS

The authors are grateful to the cyclotron crews for providing excellent quality beams and for their assistance in the preparations and measurements. The authors would like to extend their gratitude to Dr. F. Marti for insightful discussions and suggestions during the experiment.

[1] H. Ryuto, H. Hasebe, S. Yokouchi, N. Fukunishi, A. Goto, M. Kase, and Y. Yano, in *Proceedings of the 18th International Conference on Cyclotrons and Their Applications,* (INFN-LNS, Giardini Naxos, Italy, 2007), p. 314.

[2] W. Barth, in *Proceedings of the 20th International Linac Conference, Monterey, California, USA*, edited by A. Chao, eConf C000821 (2000), p. 1033 [http://www.slac.stanford.edu/econf/C000821/FR201.pdf].

[3] F. Marti, S. Hitchcock, O. Kester, and J. Oliva, in Proceedings of the 25th International Linear Accelerator Conference (Tsukuba, Ibaraki, Japan, 2010), p. 659 [http://accelconf.web.cern.ch/AccelConf/LINAC2010/papers/tup105.pdf].

[4] H. Kuboki, H. Okuno, S. Yokouchi, H. Hasebe, T. Kishida, N. Fukunishi, O. Kamigaito, A. Goto, M. Kase, and Y. Yano, Phys. Rev. ST Accel. Beams **13**, 093501 (2010).

[5] E. Baron, M. Bajard, and C. Ricaud, Nucl. Instrum. Methods Phys. Res., Sect. A **328**, 177 (1993).
[6] M. Odera, Y. Chiba, T. Tonuma, M. Hemmi, Y. Miyazawa, T. Inoue, T. Kambara, M. Kase, T. Kubo, and F. Yoshida, Nucl. Instrum. Methods **227**, 187 (1984).
[7] O. Kamigaito *et al.*, Rev. Sci. Instrum. **76**, 013306 (2005).
[8] Y. Yano, in *Proceedings of the 13th International Conference on Cyclotrons and their Applications, Vancouver, BC, Canada, 1992*, edited by G. Dutto and M. K. Craddock (World Scientific Publishing Co., Singapore, 1993), p. 102.
[9] M. Kase *et al.*, in *Proceedings of the 17th International Conference on Cyclotrons and Their Applications* (Particle Accelerator Society of Japan, Tokyo, Japan, 2004), p. 160.
[10] T. Nakagawa *et al.*, Rev. Sci. Instrum. **81**, 02A320 (2010).
[11] Y. Higurashi *et al.*, in Proceedings of the 1st International Particle Accelerator Conference (IPAC'10 OC/ACFA, Kyoto, Japan, 2010), p. 4191 [http://accelconf.web.cern.ch/AccelConf/IPAC10/papers/thpec060.pdf].
[12] J. Ohnishi, T. Nakagawa, Y. Higurashi, H. Okuno, K. Kusaka, A. Goto, and T. Minato, in *Proceedings of the 11th European Particle Accelerator Conference* (EPS-AG, Genoa, Italy, 2008), p. 433.
[13] O. Kamigaito *et al.*, in Proceedings of the 11th International Conference on Heavy Ion Accelerator Technology, Venice, Italy (2009), p. 21 [http://accelconf.web.cern.ch/AccelConf/HIAT2009/papers/mo-11.pdf].
[14] M. Kase *et al.*, in RIKEN Accel. Prog. Rep. **36**, 5 (2003).
[15] T. Kishida *et al.*, Nucl. Instrum. Methods Phys. Res., Sect. A **438**, 70 (1999).
[16] T. Mitsumoto, N. Fukunishi, A. Goto, N. Inabe, O. Kamigaito, H. Ryuto, N. Sakamoto, and Y. Yano, in *Proceedings of the 17th International Conference on Cyclotrons and Their Applications* (Particle Accelerator Society of Japan, Tokyo, Japan, 2004), p. 384.
[17] N. Inabe, N. Fukunishi, A. Goto, M. Kase, H. Ryuto, N. Sakamoto, S. Yokouchi, Y. Yano, and T. Mitsumoto, in Proceedings of the 17th International Conference on Cyclotrons and Their Applications (Ref. [16]), p. 200.
[18] ACF–Metals Arizona Carbon Foil Co. Inc. [http://www.techexpo.com/firms/acf-metl.html].
[19] B. Erb, GSI Report No. P-7-78, GSI 1978.
[20] A. Perumal, V. Horvat, R. Watson, Y. Peng, and K. Fruchey, Nucl. Instrum. Methods Phys. Res., Sect. B **227**, 251 (2005).
[21] K. Shima, T. Mikumo, and H. Tawara, At. Data Nucl. Data Tables **34**, 357 (1986).
[22] B. Franzke, Ann. Isr. Phys. Soc. **4**, 111 (1981).
[23] H. Betz, *Applied Atomic Collision Physics* (Academic Press Inc., Oak Ridge, Tennessee, 1983), Vol. 4, p. 1.
[24] A. Leon, S. Melki, D. Lisfi, J. Grandin, P. Jardin, M. Suraud, and A. Cassimi, At. Data Nucl. Data Tables **69**, 217 (1998).
[25] M. McMahan and B. Feinberg, LBL Report No. LBL-29758, 1992.
[26] K. Shima, T. Ishihara, and T. Kumo, Nucl. Instrum. Methods Phys. Res., Sect. A **200**, 605 (1982).
[27] G. Schiwietz and P. Grande, Nucl. Instrum. Methods Phys. Res., Sect. B **175–177**, 125 (2001).
[28] P. Strehl, in *Handbook of Accelerator Physics and Engineering*, edited by A. Chao and M. Tigner (World Scientific Publishing Co., Singapore, 1999), p. 555, 2nd ed.